Liquid Crystals
Publication details, including instructions for authors and subscription information:
http://www.informaworld.com/smpp/title~content=t713926090

Comparison of shear-induced conductivity anisotropy in a micellar system in the isotropic and the nematic phase

Panos Photinos[a]
[a] Department of Physics and Engineering, Southern Oregon University, Ashland, OR, USA

Online publication date: 06 July 2010

To cite this Article Photinos, Panos(2010) 'Comparison of shear-induced conductivity anisotropy in a micellar system in the isotropic and the nematic phase', Liquid Crystals, 37: 6, 695 — 700
To link to this Article: DOI: 10.1080/02678292.2010.481914
URL: http://dx.doi.org/10.1080/02678292.2010.481914

Liquid Crystals,
Vol. 37, Nos. 6–7, June–July 2010, 695–700

Taylor & Francis
Taylor & Francis Group

INVITED ARTICLE

Comparison of shear-induced conductivity anisotropy in a micellar system in the isotropic and the nematic phase

Panos Photinos*

Department of Physics and Engineering, Southern Oregon University, Ashland, OR 97520, USA

(*Received 12 December 2009; accepted 18 March 2010*)

Conductivity measurements are presented in two isotropic micellar solutions and in the nematic phase of the sodium salicylate/cetylpyridimium chloride/H_2O system under shear. For the isotropic solutions the concentrations studied correspond to the plateau behaviour in the flow curve for this system. The measured anisotropy in the shear-aligned isotropic solutions is at least one order of magnitude smaller than the anisotropy in the nematic phase. Time-resolved measurements show that the relaxation behaviour on shear start-up and on shear cessation is much faster in the isotropic solutions than in the nematic phase. The results suggest that the micelles in the shear-induced low viscosity phase are shorter than in the nematic phase.

Keywords: micellar; nematic; conductivity anisotropy; shear banding

1. Introduction

The ability to vary the shape and size of the micelles by appropriate modification of the composition and concentration has generated a wealth of phase diagrams [1, 2]. An essential factor in determining the size and geometry of the micelles is the interaction between the head groups at the surface of the micelle. Above a critical concentration, which depends on the particular amphiphile system and the temperature, spherical micelles begin to form. The critical micellar concentration (CMC) is typically a fraction of 1 mM. At high concentrations, typically of the order of 1 M or higher, a variety of smectic phases are formed, including the hexagonal, consisting of infinitely long cylinders arranged in a hexagonal packing, and the lamellar smectic phase, which consists of parallel bilayers. The smectic phases are very viscous and do not align readily in applied magnetic fields. Nematic phases can be observed in binary amphiphile/water systems, typically at about 30–50 wt%. Examples include the systems tetradecyl-trimethylammonium bromide (MTAB) in H_2O [3], decylammonium chloride (DACl) in H_2O [4], and caesium perfluorooctanoate (CsPFO) in H_2O [5]. The MTAB system gives the calamitic or N_C phase, consisting of long cylindrical micelles. The DACl and CsPFO systems give the discotic or N_D phase, consisting of disc-like micelles. The addition of salts can stabilise the nematic phase in binary systems. For example, the addition of NH_4Cl to the DACl system increases the temperature range of the N_D phase [4]. In some systems phase transitions between the N_D and N_C phases have been achieved by the addition of 1-decanol. Thus, the addition of 1-decanol in the sodium decylsulfate (SDS)/Na_2SO_4/D_2O system can induce a direct transition from the N_D to the N_C phase [1], while in the potassium laurate (KL)/H_2O system the addition of 1-decanol induces an intermediate biaxial nematic N_B phase between the N_D and N_C phases [6]. The addition of 1-decanol helps to screen the repulsive interactions between the ionic surfactant heads at the micelle-water interface, and this reduces the curvature [7].

The addition of strongly bound counter-ions in binary systems can have a major effect on the size of the micelles. As first reported by Rehage and Hoffmann [8, 9], the addition of sodium salicylate (NaSal) to the cetylpyridinium chloride (CPyCl)/H_2O system can significantly increase the length of the micelles, even at concentrations as low as a few mM. The resulting micellar lengths can be as large as 1 μm, with a dramatic effect on the viscoelastic properties of the system. The long micelles can entangle and the system behaves as a polymer solution, with the added feature that the micelles have the ability to break and reassemble.

The rheological behaviour of such systems has long been a topic of theoretical and experimental study [10–12]. A common occurrence in such systems is that the viscosity, η, becomes shear-dependent, and the shear stress, σ, versus shear rate, $\dot{\gamma}$, the so-called flow curve, is therefore non-linear. Accordingly, we speak of rheological behaviour that can be shear thinning (η decreasing with $\dot{\gamma}$) or shear thickening (η increasing with $\dot{\gamma}$). Of particular interest in the present discussion is the stress plateau exhibited by certain systems in which the flow curve becomes practically horizontal, as illustrated schematically in Figure 1 [13].

*Email: photinos@sou.edu

ISSN 0267-8292 print/ISSN 1366-5855 online

DOI: 10.1080/02678292.2010.481914
http://www.informaworld.com

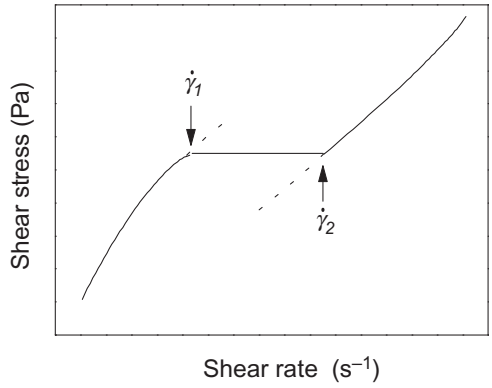

Figure 1. Model flow curve for a system showing a shear plateau. The arrows mark the first and second critical shear rates.

The plateau extends between two critical shear rates, $\dot{\gamma}_1$ and $\dot{\gamma}_2$, at the low and high ends, respectively. The stress plateau can be explained by assuming a double-value flow curve [14]. Below $\dot{\gamma}_1$ the system follows the high-shear stress branch and above $\dot{\gamma}_2$ it follows the low-shear stress branch. Between $\dot{\gamma}_1$ and $\dot{\gamma}_2$ a fraction, x, of the system follows the low-shear stress branch (lower viscosity) and a fraction $(1 - x)$ follows the high-shear stress branch (higher viscosity). At the plateau σ remains constant, and we have $\sigma = \eta_1 \dot{\gamma}_1 = \eta_2 \dot{\gamma}_2$, where η_1 and η_2 are the corresponding viscosities. Thus the plateau region reflects the coexistence of two phases with different viscosity. A simplified description of the coexistence in the cylindrical Couette cell of gap, d, involves two layers, a low viscosity layer of thickness $\sim xd$ near the moving cylinder with shear rate $\dot{\gamma}_2$, a high viscosity layer of thickness $\sim (1 - x)d$ near the stationary cylinder with shear rate $\dot{\gamma}_1$ and an interface/transition zone between the two layers. Thus, in the plateau the shear rate is not constant across the gap of the flow cell, and we therefore speak of the apparent shear rate, given by the lever rule, $\dot{\gamma} = x\dot{\gamma}_2 + (1 - x)\dot{\gamma}_1$. As demonstrated by visualisation techniques, the spatial and temporal characteristics of the coexistence regime are more complex than the two-layer description would suggest. The coexistence is potentially dominated by instabilities, slippage and chaotic dynamics at higher shear rates [15–19].

The flow curves of the CPyCl/NaSal system exhibit a robust plateau for concentrations above $\sim$ 5 wt% [20, 21]. For comparison, the CPyCl/NaSal system shows a nematic N_C phase at concentrations of $\sim$ 35 wt%. Therefore, attributing the low viscosity band above $\dot{\gamma}_1$ to a shear-induced isotropic-nematic phase transition would only appear plausible if the concentration was relatively high.

The study of the electrical conductivity has proved useful in probing the symmetry and reorientation behaviour of micellar liquid crystals [22, 23]. In particular, for the N_C phase the measurements on aligned samples show that the conductivity parallel to the symmetry axis, k_1, is larger than the conductivity perpendicular to the symmetry axis, k_2. Therefore the conductivity anisotropy, $(k_1 - k_2)$, is positive. For theoretical and numerical calculations it is convenient to introduce the reduced anisotropy

$$\alpha = (k_1 - k_2)/\langle k \rangle, \tag{1}$$

where the average value $\langle k \rangle$ is

$$\langle k \rangle = (k_1 + 2k_2)/3. \tag{2}$$

Dividing $(k_1 - k_2)$ by the average value in the definition of α given by Equation (1) eliminates the factors which affect the conductivity equally in all directions, such as ionic impurities. Experimental measurements and numerical calculations show that $\langle k \rangle$ decreases slowly as the micellar size increases. At constant temperature, therefore, α is directly proportional to $(k_1 - k_2)$. The reduced anisotropy is typically of the order of 0.1 to 0.3.

Measurements of the conductivity anisotropy in micellar systems under shear were first presented by Gotz and Heckmann [24] for an isotropic solution (19 wt%) of hexadecyl-trimethylammonium bromide (CTAB). The measurements were made for shear rates between 200 s^{-1} and 2500 s^{-1}, and the measured anisotropy was positive and found to increase with shear rate. For temperatures less than 30°C the anisotropy was saturated at the high end of the shear rate, and the values of the reduced anisotropy, α, ranged from 0.15 to 0.22. Similar measurements were reported at much lower shear rates (from 0 to 80 s^{-1}) in the less concentrated micellar system of the gemini surfactant 12–2–12 (1.5 wt%, or 1.62 mM) in D_2O [25]. The reduced anisotropy measured for this system ranged from about 0.07 at 25°C to about 0.2 at 20°C.

The present study considers conductivity anisotropy measurements for the CPyCl/NaSal system under shear. The measurements cover isotropic solutions in the concentration and shear rate ranges corresponding to the rheological plateau. An advantage of the conductivity method is that it allows measurement of the shear-induced effects in orthogonal directions separately, while the birefringence method yields the difference between refractive indices for the ordinary and extraordinary rays. The experiments presented here measure the conductivity in two geometries, parallel and perpendicular to the velocity. The measurements yield the reduced anisotropy in addition to the relaxation behaviour for each direction. The anisotropy and the relaxation behaviour provide insight into the shear-induced changes in the micellar

structure and alignment, and on the symmetry of the shear-induced low viscosity phase. The results are also compared to the anisotropy and relaxation behaviour in the shear-aligned nematic phase of the same system. The comparison shows that the anisotropy of the (potentially nematic [20]) shear-induced low viscosity band is much smaller than the reduced anisotropy in the nematic phase.

2. Experimental

2.1 Materials and sample preparation

Two isotropic solutions were prepared using CPyCl (monohydrate, from Sigma) and NaSal (from Fluka) at a molar ratio of 2 : 1 in 0.5M NaCl solution. The materials were used as received from the supplier. The concentrations of CPyCl plus NaSal in the two isotropic solutions were 6.3 wt/vol% and 21 wt/vol%, respectively. The nematic sample was prepared by mixing 32.5 wt/vol% CPyCl and 6 wt/vol% NaSal in H_2O. After mixing, the samples were allowed to equilibrate at 30°C for several days before use.

2.2 Conductivity measurements

The Couette cells used to measure the conductivity parallel to the velocity and perpendicular to the plane of shear (i.e., parallel to the long axis of the cylindrical cell) are shown schematically in Figure 2. These two directions will hereafter be referred to as parallel and perpendicular to the velocity, respectively.

The cells were constructed using precision NMR glass tubes (inner diameter 24 mm) as the outer cylinders. The inner cylinders (diameter 20 mm) were machined from Plexiglas. The cylinder spacers were machined from Teflon. Silver electrodes were painted (Colloidal silver #16034, Pelco) on the inner cylinder. To measure the conductivity parallel to the velocity, the electrodes (about 5 cm long, 1 mm wide and 10 μm thick) were deposited on the surface of the inner cylinder, diametrically opposite and parallel to the axis of the cylinder. To measure the conductivity perpendicular to the velocity, two parallel rings were deposited on the inner cylinder, spaced 5 cm apart. The outer cylinder of the cell was placed in a machined Teflon holder driven by a computer-controlled stepper motor. The applied shear rates were up to $\sim 25\ s^{-1}$. At higher shear rates, air bubbles were drawn into the electrode area and produced large fluctuations in the measurements. Periodic oscillations were also noticed, particularly in the parallel geometry matching the rotational period of the cylinders. These oscillations were of the order of $0.005\ S\ m^{-1}$ (see Figure 3) and resulted from imperfect alignment of the inner and outer cylinders of the conductivity cell.

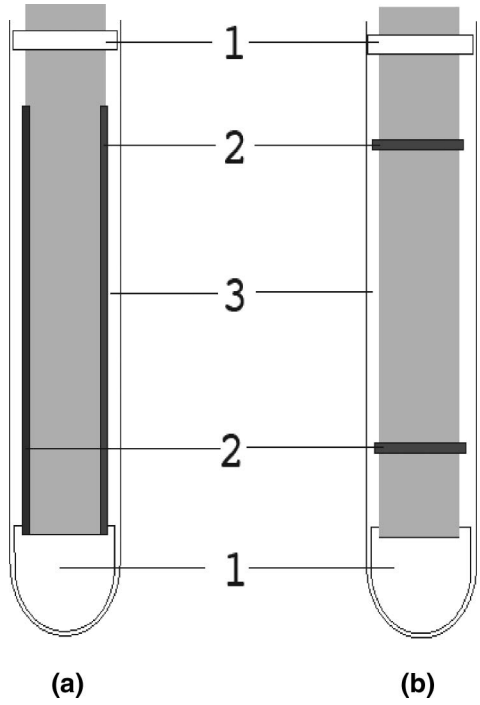

Figure 2. Cell geometry (a) for the measurement of the conductivity parallel to the velocity, and (b) for the measurement of the conductivity perpendicular to the plane of shear. *1*, Teflon spacers; *2*, silver electrodes; *3*, glass cell.

The resistance was measured using an LCR impedance meter (Stanford Research Systems, Model SR720). All of the measurements were carried out at frequency 1 kHz, and the signal amplitude was 0.1 V. The LCR meter was configured in the parallel circuit, R + Q mode, and the value of Q (ratio of imaginary

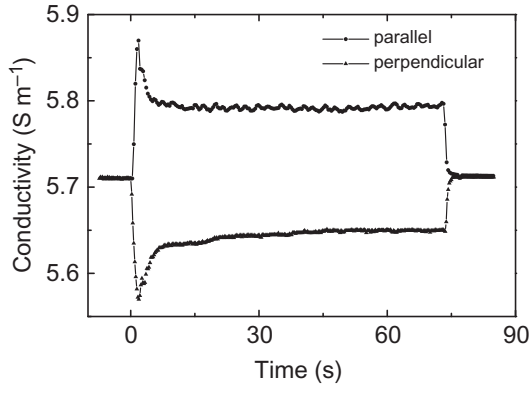

Figure 3. Conductivity components parallel and perpendicular to the velocity for the 21% sample at a shear rate $\dot{\gamma} = 6.15\ s^{-1}$. The sample was initially at rest, and the flow was started at $t = 0$ s.

to real impedance) was negative and less than 3%, indicating that the impedance of the sample was ohmic with a small capacitive component. The conductivity values were determined from the resistance measurements by calibrating the cells against a series of standard KCl solutions. The measurements were made at 25°C.

3. Results and discussion

3.1 Isotropic solutions

The conductivities parallel and perpendicular to the velocity for the 21% sample at shear rate $\dot{\gamma} = 6.15\ s^{-1}$ are shown in Figure 3. The sample was initially at rest. The shear was started at $t = 0$ s and turned off at $t = 72$ s. After an initial transient behaviour, the conductivities reached a steady state value at about 45 s. It can be seen that the two components changed in opposite directions. With reference to the conductivity at rest, the change in the parallel component was positive, whereas the change in the perpendicular component was negative. It is also noted that the transient features appeared more or less identical for both components. Similar remarks apply to all the measurements presented in this study.

These observations clearly indicate a shear-induced alignment of the micelles, with a resulting positive anisotropy, i.e., of similar symmetry to the N_C nematic phase. The initial overshoot in the parallel component (undershoot in the perpendicular component) occurred also in rheological and viscosity measurements [8, 20], and is attributed to initial stretching of the entangled micelles along the direction of motion. The overshoot is observed in the 21% sample for all shear rates above $\dot{\gamma} \simeq 2\ s^{-1}$. For the 6.3% sample the overshoot and undershoot occurred above $\dot{\gamma} \simeq 5\ s^{-1}$ and with reduced amplitude. The overshoot was not observed in the nematic sample. On cessation of shear, the sample recovered the zero shear value within a few seconds.

Figure 4 shows the reduced anisotropy as a function of applied shear rate for the 6.3% and 21% samples.

The anisotropies were determined from the steady state values of the conductivity measurements, similar to those shown in Figure 3, obtained at various shear rates. The values were calculated using Equations (1) and (2). For the calculation the conductivity measured parallel to the velocity was used as k_1 and the conductivity measured perpendicular to the velocity was used as k_2. The conductivity at rest was used as the value of $<k>$, thus referring all the values to the zero shear rate. For simplicity, it was assumed that the micelles align parallel to the velocity. Birefringence measurements in the CPyCl/NaSal system [26] show that the director of

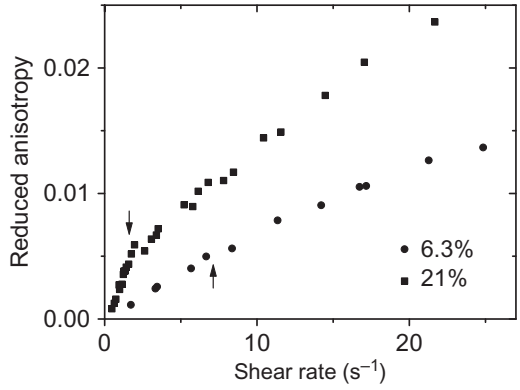

Figure 4. Reduced anisotropy as a function of the applied shear-rate for the 6.3% and 21% samples.

the shear-aligned micelles and the velocity can form an angle of about 20°, corresponding to an error of about 1% in the value of k_1. The results in Figure 4 show that the shear-induced anisotropy for the 21% sample was almost double the anisotropy induced in the 6.3% sample. The result is readily understood in terms of the higher concentration of the micelles in the 21% system. Note that the micelles in both systems are long, and the concentration in this range therefore has little effect on the micellar shape. The two arrows in Figure 4 mark the onset of the plateau as obtained from rheological measurements. The anisotropy data for the 21% sample in Figure 4 show a clear change in the slope at $\dot{\gamma} \simeq 2\ s^{-1}$, which corresponds well with the critical value, $\dot{\gamma}^1 \simeq 1.5\ s^{-1}$, obtained from the rheological measurements [20]. For the 6.3% sample the rheological data indicate a critical value, $\dot{\gamma}^1 \simeq 6\ s^{-1}$, and the conductivity anisotropy data also indicate a change in the slope, which is less pronounced than the change for the 21% sample. The data indicate that for both concentrations, as the shear rate increases above $\dot{\gamma}_1$ the incremental change in the anisotropy is smaller, i.e., the low viscosity shear-induced phase above $\dot{\gamma}_1$ has lower anisotropy. This result does not exclude the possibility of a shear-induced nematic order above $\dot{\gamma}_1$ if, for example, the micelles in the induced phase are shorter than the characteristic length of the stretched micellar sections in the more entangled highly viscous phase.

3.2 Nematic phase

Figure 5 shows the conductivity parallel to the velocity in the nematic sample, as the shear rate was ramped from 0 to 7.7 s^{-1}, with a dwell time of about 34 s at each shear rate value. The sequence of shear rates applied was: 2.6, 4.0, 5.3, 6.2, 7.3 and 7.7 s^{-1}. The arrows in the figure indicate the shear step-up points. It can be seen that the conductivity became saturated at relatively

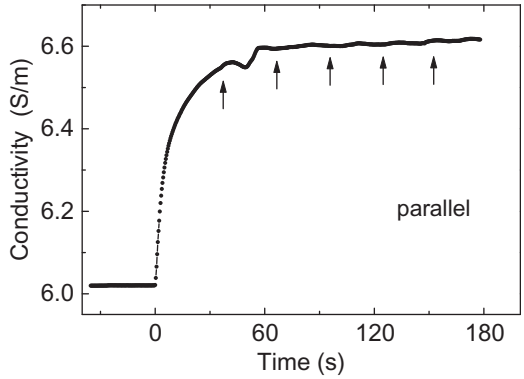

Figure 5. Conductivity parallel to the velocity in the nematic sample. The shear was increased in steps with a dwell time of about 34 s at each shear rate value. The sequence of the shear rates applied was: 2.6, 4.0, 5.3, 6.2, 7.3 and 7.7 s^{-1}. The arrows indicate the shear step-up.

low shear rates. When the shearing was stopped, the conductivity of the sample did not readily recover its initial rest value, but instead it decreased slowly over the next few hours.

This point is more clearly illustrated in Figure 6, which shows the conductivity perpendicular to the velocity. In this experiment the shear rate was ramped through a similar sequence, with a shear cessation interval between each point of the sequence. The arrows in Figure 6 indicate the shear start-up. During the intervening shear turn-off intervals, the conductivity increased slightly but remained much lower than the initial rest value. A slower relaxation over several hours occurred once the shear had been permanently turned off, but the initial value was never regained, presumably the result of anchoring the nematic director at the machined Plexiglas inner cylinder. As a result of this the nematic sample may remain in a partially aligned state indefinitely. These considerations indicate that the anisotropy values in the nematic phase may include a substantial error (as much as 50%) due to the spontaneous alignment at the cell surfaces.

The reduced anisotropy in the nematic phase is shown as a function of the applied shear rate in Figure 7. It will be noted that the anisotropy became saturated at relatively low shear rates and was one order of magnitude larger than the anisotropy of the isotropic samples at corresponding shear rates. The reduced anisotropy in the nematic phase was in good agreement with the values measured in magnetically aligned N_C nematic phases. For the N_C phase of the 25.15 KL/6.33 1-decanol/68.52 D_2O (by weight) the reduced anisotropy was $\alpha \simeq 0.15$ [27]. For the N_C phase of 36 wt% MTAB in D_2O, $\alpha \simeq 0.18$ [28].

The anisotropy values can be used to estimate the length-to-diameter ratio l/d in the nematic phase using results of numerical model calculations for the N_C phase [29]. For comparison with the numerical results, it has been assumed that the aqueous medium surrounding the insulating micelles was uniformly conducting and that the micelles were aligned rigid cylinders. Comparison with the numerical results shows that the reduced anisotropy, $\alpha \simeq 0.22$ as defined by Equation (1), corresponds to $l/d \simeq 10$. As the micelles in the nematic phase were not rigid, the value determined from the comparison physically corresponds to the characteristic length over which the alignment between neighbouring micelles persisted. Thus the average length of the flexible micelles could have been much larger.

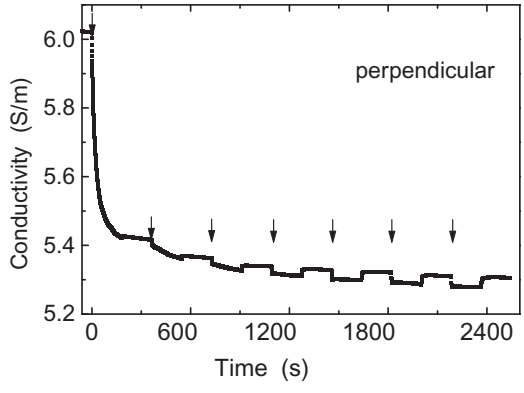

Figure 6. Conductivity perpendicular to the velocity. In this experiment the shear rate was ramped through the sequence 2.6, 4.0, 5.3, 6.2, 7.3 and 7.7 s^{-1} with a shear cessation interval between each point of the sequence. The arrows indicate the shear start-up.

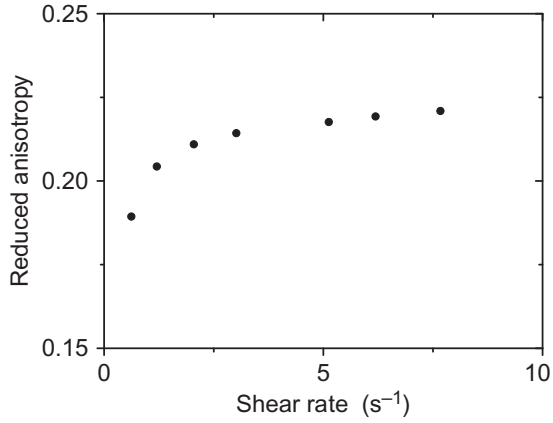

Figure 7. Reduced anisotropy in the nematic phase as a function of applied shear rate.

The relaxation behaviour of the nematic phase was considerably slower compared to the isotropic samples, not only on shear cessation, as pointed out earlier, but also on shear start-up. As seen from Figures 5 and 6, the steady state was approached more gradually, with no indication of overshoot/undershoot transients. These differences suggest that the micellar structure of the shear-induced low viscosity phase differed from the structure in the nematic sample. The difference in the relaxation behaviour was consistent with the conclusions supported by the anisotropy behaviour mentioned in the preceding subsection, namely shorter micellar lengths for the shear-induced low viscosity phase.

4. Conclusions

Conductivity measurements can be a useful tool in investigating the symmetry and realignment of micellar systems under shear. For the shear-aligned isotropic micellar solutions of the CPyCl/NaSal system, the conductivity measurements show that the symmetry of the shear-induced low viscosity phase is similar to the N_C nematic phase. Comparison with anisotropy and relaxation behaviour in the nematic phase suggests that the micelles in the shear-induced phase are shorter than those in the nematic phase.

Acknowledgements

The continued presence of Alfred Saupe is gratefully acknowledged, together with his enrichment of the author's professional, personal and spiritual life.

References

[1] Saupe, A. *Nuovo Cimento* **1984**, *3*, 16–29.
[2] Forrest, B.J.; Reeves, L.W. *Chem. Rev*. **1981**, *81*, 1–14.
[3] Saupe, A.; Xu, S.Y.; Plumley, S.; Zhu, Y.K.; Photinos, P. *Physica* **1991**, *174A*, 195–207.
[4] Rizzatti, M.R.; Gault, J.D. *J. Colloid Interface Sci*. **1986**, *110*, 258–262.
[5] Boden, N.; Corne, S.A.; Jolley, K.W. *J. Phys. Chem*. **1987**, *91*, 4092–4105.
[6] Yu, L.J.; Saupe, A. *Phys. Rev. Lett*. **1980**, *45*, 1000–1003.
[7] Charvolin, J. *J. Chim. Phys*. **1983**, *80*, 15–23.
[8] Rehage, H.; Hoffmann, H. *Rheol. Acta* **1982**, *21*, 561–563.
[9] Rehage, H.; Hoffmann, H. *J. Chem. Phys*. **1988**, *92*, 4712–4719.
[10] Cates M.E.; Fielding, S.M. *Adv. Phys*. **2006**, *55*, 799–879.
[11] Manneville, S. *Rheol. Acta* **2008**, *47*, 301–318.
[12] Callaghan, P.T. *Rheol. Acta* **2008**, *47*, 243–255.
[13] Berret, J.F. In *Molecular Gels*: Weiss, R.G., Terech, P., Eds.; Springer: Dordrecht, 2005; pp 235–275.
[14] Spenley, N.A.; Yuan, X.F.; Cates, M.E. *J. Physique II* **1996**, *6*, 551–571.
[15] Lerouge, S.; Argentina, M.; Decruppe, J.P. *Phys. Rev. Lett*. **2006**, *96*, 088301.
[16] Lerouge, S.; Fardin, M.A.; Argentina, M.; Grégoire, G.; Cardoso, O. *Soft Matter* **2008**, *4*, 1808–1819.
[17] Fardin, M.-A.; Lasne, B.; Cardoso, O.; Grégoire, G.; Argentina, M.; Decruppe J.P.; Lerouge, S. *Phys. Rev. Lett*. **2009**, *103*, 028302.
[18] Fielding S.M.; Olmsted, P.D. *Phys. Rev. Lett*. **2004**, *92*, 084502.
[19] Fielding S.M.; Olmsted, P.D. *Phys. Rev. Lett*. **2006**, *96*, 104502.
[20] Berret, J.-F.; Roux, D.; Porte, G. *J. Physique II* **1994**, *4*, 1261–1279.
[21] Berret, J.-F.; Porte, G.; Decruppe, J.-P. *Phys. Rev*. **1997**, *E55*, 1668–1676.
[22] Winsor, P.A. In *Liquid Crystals and Plastic Crystals*: Gray, G.W., Winsor, P.A., Eds.; Vol. 2; Ellis Horwood: Chichester, 1974; pp 122–143.
[23] Photinos, P. In *Phase Transitions in Complex Fluids*: Toledano, P., Neto, A.F., Eds.; World Scientific Publishing: Hackensack, NJ, 1998; pp 173–195.
[24] Gotz, K.G.; Heckmann, K. *J. Colloid Sci*. **1958**, *13*, 266–272.
[25] Oda, R.; Panizza, P.; Schmutz, M.; Lequeux, F. *Langmuir* **1997**, *13*, 6407–6412.
[26] Lee, J.Y.; Fuller, G.G.; Hudson, N.E.; Yuan, X.-F. *J. Rheol. (Melville, NY, US)* **2005**, *51*, 537–550.
[27] Photinos, P.; Melnik, G.; Saupe, A. *J. Chem. Phys*. **1986**, *84*, 6928–6932.
[28] Photinos, P.; Xu, S.Y.; Saupe, A. *Phys. Rev. E: Stat., Nonlinear, Soft Matter Phys*. **1990**, *42*, 865–871.
[29] Photinos, P.; Saupe, A. *Mol. Cryst. Liq. Cryst*. **1983**, *98*, 91–97.